Foundations of Science
https://doi.org/10.1007/s10699-022-09890-w

Nomograms in the History and Education of Machine Mechanics

Giovanni Mottola[1] · **Marco Cocconcelli**[1]

Accepted: 20 November 2022

Abstract
Computing formulae and solving equations are essential elements of scientific analysis. While today digital tools are almost always applied, analog computing is a rich part of the larger history of science and technology. Graphical methods are an integral element of computing history and still find some use today. This paper presents the history of nomograms, a historically-relevant tool for solving mathematical problems in various branches of science and engineering; in particular, we consider their role in mechanical engineering, especially for education, and discuss their mathematical properties. Each nomogram is a graphical description of a specific mathematical equation, designed such that the solution can be found through a simple geometric construction that can be performed with a straightedge. By design, using nomograms requires little skills and can be done even in adverse environments; a solution of sufficient accuracy for most purposes can then be found in a very short time. Another important advantage of nomograms is that they offer clear insight on the relationships between the variables, an insight which can be lost by looking at a complex equation. First introduced in the late 19th century, nomograms were used by engineers and scientists due to their speed with respect to manual calculations, before being superseded by computers. While now mostly obsolete in practice, nomograms can still prove useful in workshops and teaching classes: we thus also discuss their educational applications and present a few original examples.

Keywords Nomograms · History of machines and mechanisms · Mechanical engineering education · Graphical computing · Mechanics of machines

This paper is an extended version of our work *"Nomograms: an old tool with new applications"* presented at the "*7th International Symposium on History of Machines and Mechanisms (HMM 2021)*", Jaén, Spain, 28-30 April 2022.

✉ Giovanni Mottola
giovanni.mottola@unimore.it

[1] Department of Sciences and Methods for Engineering, University of Modena and Reggio Emilia, Via G. Amendola 2, 42122 Reggio Emilia, Italy

1 Introduction

In science and engineering, the analysis of a specific problem frequently leads to a physical model, which in turn provides one or more mathematical equations to be solved. Commonly, these equations correlate several scalar parameters, so that a subset of them can be derived as functions of the other ones: consider, for instance, the parameters for the design of a mechanical component with respect to the input constraints. We are interested in equations that have a finite number of solutions, which can then be computed; in other words, we disregard equations which define a multi-dimensional boundary (with infinitely many points).

For all but the simplest equations found in practice, the solution process requires some computational device, as the mathematical steps are usually tedious (or even prohibitively long) to perform by hand. In fact, large research centers such as NASA used to hire teams of human computers, who were assigned a list of arithmetical operations to be performed (Grier, 2001). Hand calculations, however, have a high risk of errors, where all the results after a single mistake may be invalid: this is due also to the lack of insight over the intermediate results, which are often difficult to check.

An alternative once in common use are *graphical methods*, some of which have been known since antiquity. These methods are defined by the tools used, such as writing devices, straightedges and compasses: the mathematical problem is then turned into an equivalent geometrical problem, which is solved by a corresponding construction. Due to their design, graphical methods can be much faster than analytical procedures; moreover, they are generally more intuitive to understand, even for users with limited mathematical proficiency. Finally, the visualization of the data is intrinsic in the solution process: this makes it easier to spot potential errors, but also provides insight over the relationships between the parameters. On the other hand, graphical methods have fixed accuracy (due to the tools used and to the manual dexterity of the user), which is however more than sufficient in most cases.

For the advantages outlined above, graphical methods used to be (and, in part, still are) commonly used by researchers, particularly in engineering education and practice, where larger approximations are acceptable. However, they have now been largely surpassed by digital methods: the advent of personal computers in the latter half of the 20th century made large-scale computations affordable and immediate and general-purpose software for equation solving is now a default tool for these problems. Nevertheless, graphical methods are still worth studying, if nothing else as part of the broader history of science and as teaching tools to introduce complex concepts.

Among other graphical tools, *nomograms* (d'Ocagne, 1899) are systems of *scales* (that is, parametric curves in one variable), designed in such a way that the mathematical relationship between the variables can be equivalently expressed in a simple geometric form, such as the collinearity of three points. Therefore, a nomogram can be used to solve an equation by choosing the variables that are designed as inputs and marking the corresponding point on the respective scales; the solution is then found by a geometrical construction which can be performed by tools such as a straightedge[1]. Due to their advantages, nomograms used to be a staple of engineering practice, together with devices such as slide rules.

[1] Sometimes, thin threads of wire may be used to mark lines, to allow reusing the nomogram after each calculation.

We are especially interested in their role within the field of mechanical engineering, a role that we will discuss through our bibliographic research.

While no longer common today, nomography still has its applications, for instance where digital tools such as spreadsheets would be inconvenient: considering for instance shop-floor operations and open-field research, printed nomograms appear interesting due to their ruggedness and portability. Moreover, nomography can be used as a teaching tool, which helps to explain complex topics through a clear visualization.

In this paper, we aim to present the history of nomography from an engineers' perspective, in particular within the field of Mechanisms and Machine Science. We thus discuss the development of nomograms and their historical precursors, together with the mathematical research on the properties of nomograms. We also present a few original examples that we created to show possible applications of nomograms for educational purposes and to discuss guidelines in the development of such tools. We believe that similar examples can be useful both for inspiring interest among engineering students towards the history of our discipline and to elucidate mathematical concepts that would be otherwise difficult to visualize. In our work, we used the open-source nomographic library *pyNomo* (Boulet et al., 2020), developed in the Python programming language, to create visually attractive graphs (as high-quality vector images) in an automated way that is much quicker than traditional manual approaches.

The remainder of this paper is structured as follows. In Sect. 2, we discuss the history of nomography, with a focus on their application in mechanical design. We then present the mathematical properties of nomograms and the methods to design new ones in Sect. 3; we also discuss how simple nomograms can be combined to solve equations of several variables. Later, in Sect. 4, we present selected nomograms and their potential industrial and educational applications; these nomograms are original (to the best of our knowledge) and useful to understand the advantages and limitations of these tools. Finally, we offer our conclusions and directions for future work in Sect. 5.

2 Nomograms in History

For more than a century, nomograms were researched by mathematicians and taught in technical education programs. Due to their past significance, nomograms were analyzed in terms of their historical development in several review works, such as Doerfler (2009), Evesham (1986, 2010), Hankins (1999), Tournès (2003); however, to the best of our knowledge, no such reviews have been presented from the perspective of engineers.

To define the scope of our research, we only consider purely graphic approaches that require nothing more than pencil and straightedge. Thus, we disregard approaches that use complex mobile elements: for instance, we will not discuss the role of *slide rules*, another instrument (conceptually related to nomograms) that was in use until the '60s.

We remark that the terminology is not unequivocal: several works on "nomograms" use in fact graphical methods that are quite different—and generally more cumbersome to use—than standard nomograms (Grimes, 2008), such as graphs having one or more lookup curves with data from experiments or previous calculations. Here, instead, we only consider methods that require some geometrical construction. Moreover, especially in older sources, alternative terms such as "nomographs", "alignment charts" and "abacs" are used interchangeably (Doerfler, 2009). To avoid confusion, in this paper we always use the term "nomogram", first introduced by French mathematician and engineer Maurice d'Ocagne

(1862–1938) in the late 19th century (d'Ocagne, 1899) to distinguish his work from previous contributions: our bibliographic search on scholarly research engines shows that this expression remains the prevalent one.

2.1 Invention and Diffusion: 1800–1960

Nomogram (from the Greek νόμος, meaning "law", and γραμμή, meaning "line") is a relatively recent term, which should not be applied to tools preceding the work by d'Ocagne (Evesham, 1986); still, d'Ocagne was influenced by other authors, from whose we can understand the main concepts of nomography as he developed it.

Mechanical devices for computation have been developed since antiquity, where movable parts represent numbers and their relationships. An example is the *abacus*, using beads moving on wires. Devices that can be seen as precursors to nomograms are:

1. *Astrolabes* and *equatoria* (Evesham, 1986; Tournès, 2003), for computing the positions of the Sun, the Moon and the planets; e.g. Richard of Wallingford's *Albion* (1300s) and the *jovilabe* (1600s) used by Galilei to study the moons of Jupiter.
2. *Sundials* (Evesham, 1986; Glasser and Doerfler, 2019) and *moondials* (Tournès, 2003); like nomograms, these are based on calculations and present results graphically.
3. *Volvelles* and *slide charts* (Evesham, 1986), akin to slide rules; these are made of movable pieces of paper and are designed for a specific computation.

The first tool for d'Ocagne was *coordinate geometry*, developed in the 17$^{\text{th}}$ century by French mathematician René Descartes (1596–1650): this allows us to draw the graph of a function F. We will consider mostly equations in three variables, such as

$$F(v_1, v_2, v_3) = 0 \tag{1}$$

We now define auxiliary functions F_i, each depending on the variables of interest v_i and on the coordinates x and y on a Cartesian plane, such that Eq. (1) is equivalent to

$$\begin{cases} F_1(x, y, v_1) = 0 \\ F_2(x, y, v_2) = 0 \\ F_3(x, y, v_3) = 0 \end{cases} \tag{2}$$

Three families of parametric curves can be graphed in the x-y plane, one for each F_i. Each curve is the set of points satisfying one equation in (2), for a fixed v_i; each family is thus a set of level curves for the corresponding equation. A point at the intersection of three curves (one for each family) is then a solution to Eq. (1). Expressing Eq. (1) in the form (2) is an *undetermined* problem, as there are in general infinitely many choices for the equivalent system; the choice of the F_i in (2) is guided by convenience or mathematical insight. In practice, the sets of level curves are discretized (to avoid cluttering), so no exact intersection is found; we then pick the curves corresponding to the values of the input variables (which may be any two of the v_i's) closest to the theorical ones and find the final result from graphical interpolation. Some of the main features of nomograms can already be recognized in this simpler concept, as follows.

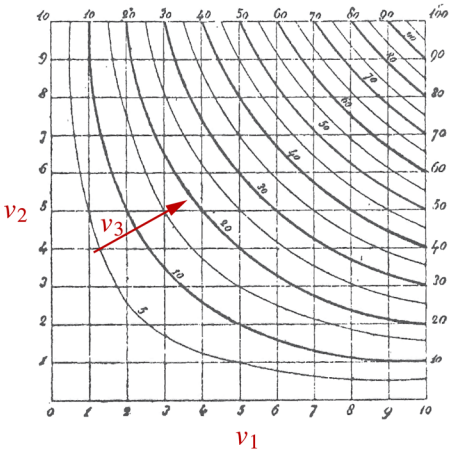

(a) Intersection nomogram.

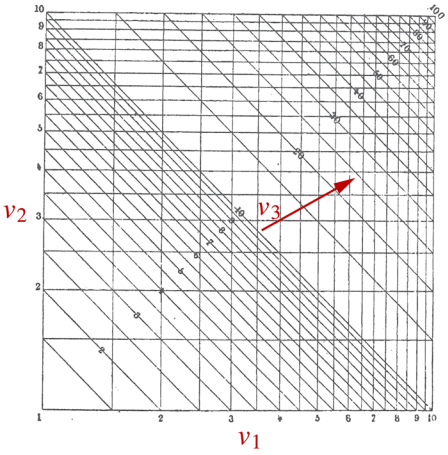

(b) Intersection nomogram with logarithmic scales.

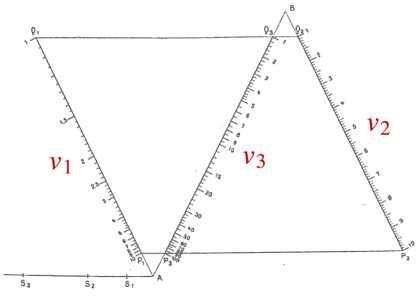

(c) Alignment nomogram, first version.

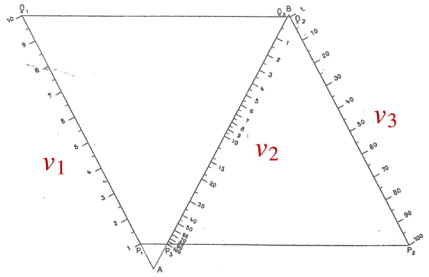

(d) Alignment nomogram, second version.

Fig. 1 For the same task (calculating the product $v_3 = v_2 v_1$) different charts can be drawn; an alignment nomogram offers an elegant solution. This can be drawn in different ways; the one in Fig. 1d has two linear scales (which are easier to draw). Charts from d'Ocagne (1899), with some changes for clarity

- From two v_i chosen as inputs, the third one can be found graphically, even if Eq. (1) is not analytically invertible; *direct* and *inverse* problems are thus equivalently easy.
- The *approximation* of a given solution is related to its distance from the closest curve of the output variable, thus providing a visual feedback of the error.
- The *accuracy* is limited by the graph resolution and by the user's skills; however, large errors due to misreading are unlikely and out-of-scale errors are impossible, since we only plot the curves corresponding to meaningful ranges for the v_i's.
- Each graph is targeted for a *specific* equation, while other calculating devices (such as slide rules) are more general; however, the method presented above is *general* and a graph can be devised for almost any equation found in practice.

If, in Eq. (2), we take for simplicity $F_1 = v_1 - x$, $F_2 = v_2 - y$ and $F_3 = F$, the graph is obtained by drawing the level curves (called *isopleths*) for constant values of F. An example is shown in Fig. 1a, for $F = v_3 - v_2 v_1 = 0$; this graph can be used to compute the product v_3 of two variables. This is in fact the first known application of this concept (also called an *intersection nomogram*), presented by French manufacturer Louis-Ézéchiel

Pouchet (1748–1809), who generalized the *discrete* multiplication tables (known from Pythagoras) as *continuous* (hyperbolic) curves. Multiplying non-integer numbers is also possible by interpolation. Pouchet's work is also historically significant as he introduced the expression "graphical calculus" (Tournès, 2000).

An issue of this method is that it requires graphing curves on paper, which in Pouchet's time was a time-consuming task done by hand. An improvement was suggested by French engineer Léon-Louis Lalanne (1811–1892), namely using *nonlinear* scales. Consider the multiplication graph in Fig. 1a: the isopleths are given by $v_1 v_2 = C$, where C is a constant. If v_1 and v_2 are reported on logarithmic axes, the graph can be simplified: the equation for the isopleths becomes $\log(v_1) + \log(v_2) = \log(C)$, so the isopleths become straight lines. The graph in Fig. 1b shows the result (compare with Fig. 1a). While drawing nonlinear scales is more complex, the convenience of drawing straight lines more than compensates this drawback, as only two points need to be found for each line. Lalanne called his concept *anamorphosis*, a painting technique using deliberately exaggerated projective distortions. Nonlinear scales became then an essential tool in devising simple nomograms for complex equations.

The final elements in this development were introduced by d'Ocagne in several works on graphical calculus in the late 1800s, culminating in the first book (d'Ocagne, 1899) on nomography proper. There, d'Ocagne also used *projective geometry*, a branch recently introduced by French engineer and mathematician Jean-Victor Poncelet (1788–1867) and others. By the principle of *duality* of points and lines, each line in an anamorphic graph is represented by a point; the condition of having three curves through a common point corresponds then to having three points aligned on a line. This simplifies the nomogram, which is much less cluttered: one only needs to draw a straight line through two points, whose positions are given by the inputs, to find the third point, providing the output. Another idea of d'Ocagne was substituting the orthogonal coordinate axes with curves $\mathcal{C}_i$ ($i = 1, 2, 3$) in the plane, thus introducing *alignment nomograms*. Each v_i defines a point P_i on curve $\mathcal{C}_i$, which is graded along its length; the scale may be linear or nonlinear (Fig. 1c and d), to make the resulting nomogram simpler to draw and to use. The points are defined parametrically as $P_i(v_i) = \left(f_{ix}(v_i), f_{iy}(v_i)\right)$ in the Cartesian plane; the condition for alignment is

$$\begin{vmatrix} f_{1x}(v_1) & f_{1y}(v_1) & 1 \\ f_{2x}(v_2) & f_{2y}(v_2) & 1 \\ f_{3x}(v_3) & f_{3y}(v_3) & 1 \end{vmatrix} = 0 \tag{3}$$

(the determinant is equal to the area of triangle $\triangle P_1 P_2 P_3$ and is zero if the points are aligned). If Eq. (1) can written in this form, then a nomogram can be found for solving it.

We remark here in passing that nomogram scales are always based on parameterized curves, as shown for instance in Eq. (3), in which each curve $\mathcal{C}_i$ depends on an independent parameter v_i. The development of parametric geometry is also interlinked to technical drawing, as indicated by the works of French mathematician Gaspard Monge (1746–1818), who opened the field of descriptive geometry (Hankins, 1999); this later became the basis for modern engineering drawing. Later still, parametric modeling became an essential component of graphical programs such as those for Computer-Aided Design (CAD), in which curves and surfaces are defined parametrically.

Alignment nomograms can also solve equations four or more variables; for instance, to solve $F(v_1, v_2, v_3, v_4, v_5) = 0$, one may first find v_3 from v_1 and v_2, and then v_5 from v_4 and the v_3 thus obtained. The two nomograms (one for each step of the solution) can then be combined, with a curve $\mathcal{C}_3$ common to both. Writing an equation in this form is difficult

in general (and not always possible), but the resulting nomogram is easier to use and understand than an intersection nomogram. Here, too, the representation of an equation is not unique: with a different scaling (such as using logarithmic scales), the nomogram is defined by different curves. One can also multiply the matrix in Eq. (3) by another constant matrix, and then take the determinant: geometrically, this is equivalent to a linear transformation in the plane (such as scaling, rotating, translating, stretching or shearing) and gives another nomogram that still solves the original equation (but may be easier to use). Creating nomograms required skill and experience in d'Ocagne's time, a limitation that can now be overcome through software (Boulet et al., 2020).

D'Ocagne's role has also been debated: some contemporaries, such as French geophysicist Charles Lallemand (1857–1938) and engineer Rodolphe Soreau (1865–1935) resisted his terminology, arguing that nomograms were merely an extension of abacs (Soreau, 1902), but we believe that d'Ocagne's contributions, especially applying projective geometry, essentially introduced a novel tool (Tournès, 2003, pp. 73–74).

After the publication of his seminal book, D'Ocagne greatly helped to popularize his invention through many later works, in which he presented example nomograms for several applications, such as physics, hydraulics, topography, navigation (Fig. 2), aviation and accounting (Tournès, 2003). By the 1920s, nomograms had become the main research topic in graphic computing (Tournès, 2000, p. 142, Fig. 3); moreover, they were the object of research interest also for their mathematical properties. For example, German mathematician David Hilbert, in his famed list (Hilbert, 1901) of 23 important open problems in mathematics, posed the 13th one in terms of nomographic analysis, by asking whether a 7th-degree polynomial equation, which cannot be solved in closed form through algebraic functions, can be solved instead through nomograms. A solution was found by d'Ocagne himself; however, the solution required a movable element in addition to a nomogram and was thus deemed unsatisfactory by Hilbert, who conjectured that the problem could not be solved in nomographic terms. Hilbert's conjecture was finally disproved in 1957 (Tournès, 2014) by Russian mathematicians Andrej Kolmogorov (1903–1987) and Vladimir Arnol'd (1937–2010).

Another research topic was to determine whether a given equation of three variables can in fact be solved through nomograms, and if so, to find a procedure for creating them: this problem was finally solved in a practical form by Polish mathematician Mieczyslaw Warmus (1918–2007), who also presented (Warmus, 1959) a classification of the functions that can be written in nomographic form into seven principal cases.

By the 1950s, research in nomography, at first mostly published in French (Tournès, 2000, p. 141, Fig. 2) after the pioneering works by Pouchet, Lalanne and d'Ocagne, had become of interest at the global level; one can observe, for example, a significant amount of works by authors from the former Soviet Union (Evesham, 1986).

Regarding Machine Design and Machine Mechanics in particular, we observe that nomograms were frequently proposed in technical magazines aimed at the practitioner, to facilitate application of theoretical results known from scientific works; general introductions to nomography were also provided (Rusconi, 1962), to explain how nomograms could be derived and used. A comprehensive catalog of about 700 references on nomograms was presented in Adams (1950), covering topics from mathematics to food preservation; in this work, 127 references were listed on Machine Design alone, published from 1920 to 1948. Example applications included the design of pressure vessels, rolling and plain bearings, rubber or helical springs, threaded fasteners, plane belts, shafts, wrapping-band brakes, planetary gear reducers, gear teeth, cams and flywheels; others were for computing natural frequencies of components such as springs or shafts. A frequent topic is also the estimation

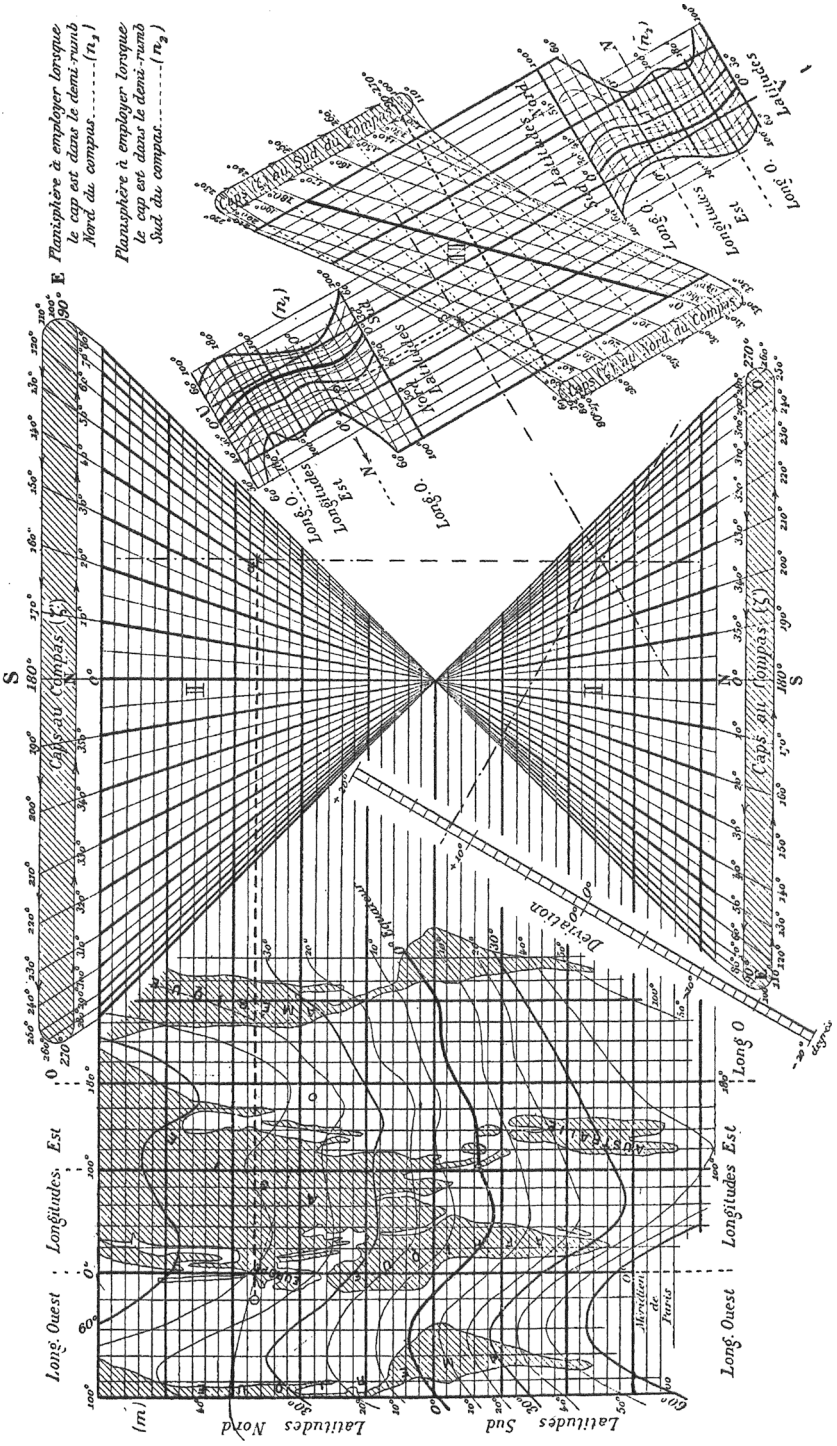

Fig. 2 An example from d'Ocagne (1899) of a complex nomogram, to compute the deviation of a compass on a ship depending on the latter's geographic coordinates

of costs for machine shop operations or raw stock; these correspond to mathematically simple yet tedious calculations that needed to be updated frequently, hence the usefulness of a dedicated tool such as a nomogram instead of slide rules or other general devices.

2.2 Decline: 1960–1990

The research on nomography began to decline in the 1960s (Tournès, 2000, p. 140, Fig. 1), as computers became commonly used in academia and industry. Nevertheless, nomograms remained in use, and published papers frequently presented calculations in nomographic form for practical applications; books and papers were written on the art of nomography and its potential uses (Bond, 1948; Ferrara, 1940). Topics that saw a significant use of nomograms are the analysis of internal combustion engines, manufacturing technology, design of hydraulic systems and civil engineering (especially for the study of soil mechanical properties). In all these cases, one needs to work with complex relationships that are often approximations of numerical data, thus the reduction in accuracy for a graphical approach (with respect to an analytic one) is not an issue. On the other hand, the possibility of quickly obtaining a result that can be used even in field work makes nomograms appealing for these applications.

Regarding applications in Machine Mechanics, we observe that until the ’70s nomographic solutions for mechanism design problems were appreciated for their practicality: indeed, mechanism design generally leads to complex equations in which it is convenient to explore different design solutions, by designating different parameters as outputs. In particular, Adams (1960) developed a nomogram to optimize a four-bar linkage for function generation and observed how, after some practice, one can arrive in a relatively short time at a suitable solution with acceptably small errors. As it was common, the nomogram was available in large format on graph paper for practical use.

Other nomograms were developed during this period specifically for mechanism design; for instance, planar four-bar mechanisms were studied in Antuma (1978) and Wunderlich (1980), while Meyer zur Capellen, W. (1983) considered their spherical equivalents. A planar mechanism with a contact pair, namely a cam-follower linkage, was studied in El-Shakery and Terauchi (1984) with the goal of preventing undercut. We also cite Éidinov et al. (1976), on the vibration analysis of a spatial (Hooke’s) joint.

Nomograms proved useful also in the design of gears (Seireg and Houser, 1970; Wellauer and Holloway, 1976) to present large amounts of experimental data in a form that is more convenient for designers than numerical tables. Some applications were also proposed for vibration analysis (Hohenberg, 1967; Miconi, 1987).

2.3 Resurgence? 1990–Today

After the ’90s, nomograms have largely disappeared from engineering research, having been replaced by software that can be easily distributed. Nevertheless, nomograms are still present in published literature: for instance, they are still used in design standards and manufacturers’ catalogs, to present results in a compact way. A common example is the Smith chart (Howison, 2014), used in electrical engineering for the design of transmission lines: in its essence, this graphical tool is again a nomogram.

It is worth observing that the visualization concepts that were promoted by the development of nomography, such as using graded scales to show relationships between data (especially large-dimensional data sets), have found use in modern tools such as web

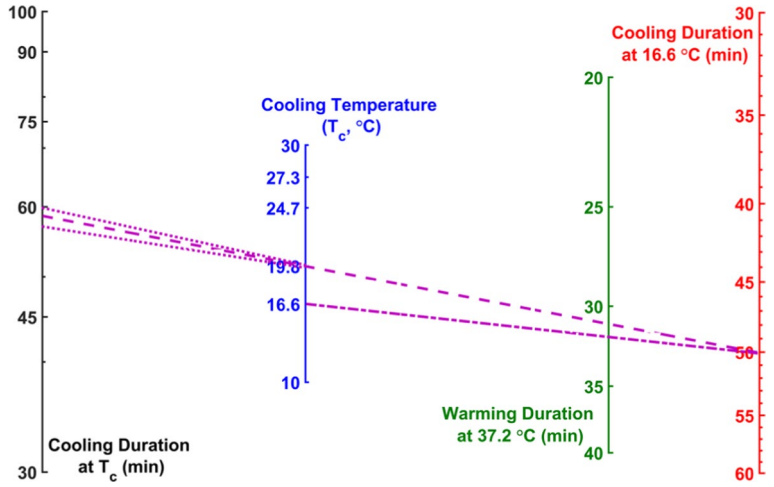

Fig. 3 Nomogram for the design of a thermal therapy protocol for soft tissue injuries. The dotted lines on the left delimit the uncertainty zone for the result. Reprinted with permission from Khoshnevis et al. (2018)

visualization systems to report statistical data: while not nomograms in the strict sense, these "smart" diagrams combine the ease of visualization of nomography with data analysis functions for easy filtering and searching. They can also be used as online calculators, emphasizing the interactive aspects of computing. A similar visualization tool are parallel coordinate plots (Wegman, 1990), which display the data in the same way as nomograms, but without defining a corresponding geometrical relationship.

Outside of engineering, nomograms have also had a significant impact on medicine (Grimes, 2008; Kattan and Marasco, 2010; Khoshnevis et al., 2018) see the example in Fig. 3. Nomograms are also used to quickly compute the BMI of a patient (Glasser and Doerfler, 2019). Their use in medicine is in fact somewhat controversial; however, even in a review (Grimes, 2008) that strongly criticized their usage as anachronistic, the author admitted that nomograms were undergoing a "resurgence", with more than 150 citations on the PubMed database in 2007 alone. Nomograms, indeed, can be helpful in explaining a complex situation to a patient (Kattan and Marasco, 2010), especially in comparison to PC programs, which may be perceived as less transparent. Nomograms are also low-cost and easily protected from environmental damage (by using waterproof paper); moreover, they allow users to compute results in emergency situations. These advantages can also be useful for engineers in some industrial applications.

Finally, nomograms can still have a place where speed is of the essence: for example, they are used to predict the behavior of forest fires or the lift of hot-air balloons (Glasser and Doerfler, 2019). Another relevant application is artillery, in which nomograms were in standard use up to World War I (Hankins, 1999). Nomograms have also been proposed for estimating seismic hazard (Douglas and Danciu, 2020).

Considering the field of Machine Mechanics and Design over the last 30 years, we found several works on nomograms for gear train design (Esmail & Hussen, 2010; Esmail, 2013, 2016; Esmail et al., 2018); they are also still used for the design of planar (Hassaan, 2015) or spherical (Hwang and Chen, 2007; Lu, 1999) linkages, for optimizing motion laws in cams (de Freitas Avelar et al., 2021), for the analysis of the efficiency of a kinematic chain

(Aleksandrov, 2011), for studying tire dynamics in a vehicle (Zotov and Balakina, 2007), and for the design of hollow springs (Bagaria et al., 2017).

3 Nomograms: Methods and Properties

In this Section, we briefly describe how nomograms can be drawn, using modern tools, for a few example problems in Machine Mechanics. While a complete guide on drawing nomograms (Doerfler, 2009) is beyond the scope of this work, we believe that some example nomograms can effectively show the advantages and limitations of these tools.

3.1 Modern Nomographic Tools: pyNomo

Traditionally, a notable limit of nomograms is that they require considerable skill in their design, not to mention the time needed to manually draw them in high detail. Recently, however, some software tools have been presented (Howison, 2014) that allow us to automate nomogram design: these tools can help reintroduce nomography in practical usage. Indeed, as observed in Kattan and Marasco (2010), it is desirable to have a tool that *"combines computerization with classical nomograms"*. At the time of writing, the most complete software for this task (that we are aware of) is pyNomo (Boulet et al., 2020), a library for nomography written in the Python programming language. Therefore, we have created a few nomograms with pyNomo to illustrate some basic concepts in Machine Mechanics. A pyNomo script, once it has been run, generates and automatically compiles (through Python) a LaTeX source-code file; the final output is a PDF file containing the nomogram in high-quality vector graphics.

3.2 Selected Nomogram Types

In this work, we refer to the classification in the pyNomo documentation (Boulet et al., 2020), whose authors identify 10 types of nomograms (Martínez-Pagán and Roschier, 2022). Traditionally, the most common nomogram is the one defined by three parallel[2] straight lines (Type 1 in pyNomo[3]); an example of this design is in Fig. 4. The most general mathematical expression for an alignment nomogram, as defined in Eq. (3), becomes simpler in this case: having defined a coordinate system with axis x parallel to the scales, the j-th scale (along the line $y = y_j$) starts at $x = x_{jS}$ and ends at $x = x_{jE}$ ($j = 1, 2, 3$), therefore we can write

$$\begin{cases} f_{jx}(v_j) = x_{jS} + \Delta x_j g_j(v_j) \\ f_{jy}(v_j) = y_j \quad \text{(constant)} \end{cases} \quad \text{with} \quad \begin{cases} g_j(v_{jS}) = 0 \\ g_j(v_{jE}) = 1 \end{cases} \quad \text{and} \quad \Delta x_j = x_{jE} - x_{jS} \tag{4}$$

[2] In most nomograms of this type, the lines are vertical, for clarity. Here the lines are horizontal, to save space.

[3] In this paper, we follow the same terminology and classification proposed in Boulet et al. (2020), for clarity.

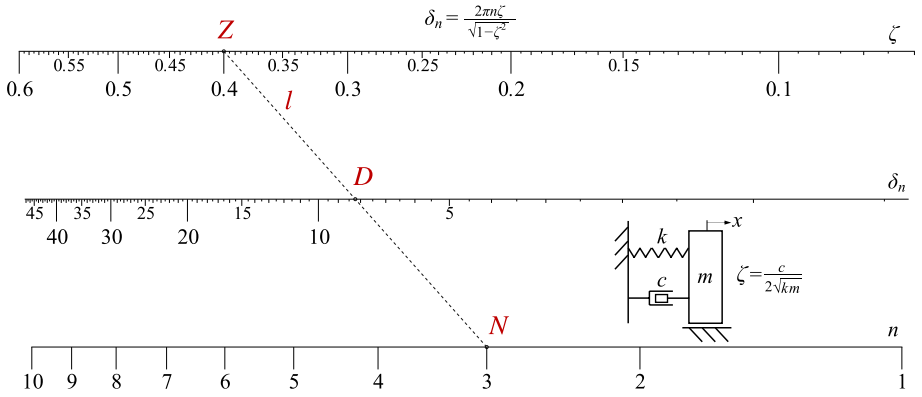

Fig. 4 Nomogram for the logarithmic decrement δ_n of a mass-spring-damper system, defined as $\delta_n = \log\left(x_1/x_{n+1}\right)$, where x_i is the amplitude of the i-th oscillation after release from an initial displacement (without external forces). Points Z, D and N are defined by the values $\zeta = \frac{c}{2\sqrt{km}}$ of the damping ratio, δ_n of the decrement and n of the number of oscillations for defining δ_n, respectively (each on the corresponding scale); c, k and m are the damping coefficient, the stiffness and the mass. The points are aligned on line l

where $v_j \in \left[v_{jS}, v_{jE}\right]$ is the j-th variable, defining a point on the corresponding scale, and g_j is a suitable monotonic continuous function; for example, setting $g_j(v_j) = \frac{v_j - v_{jS}}{\Delta x_j}$ defines a uniform linear scale. Substituting in Eq. (3), one has

$$\left(y_3 - y_2\right)\Delta x_1 g_1(v_1) + \left(y_1 - y_3\right)\Delta x_2 g_2(v_2) + \left(y_2 - y_1\right)\Delta x_3 g_2(v_3) + C_0 = 0 \tag{5}$$

where C_0 is a constant depending on the parameters of the nomogram. This shows that any *weighted sum* of functions g_j can be computed with a nomogram such as the one shown in Fig. 4; the weights $\left(y_i - y_k\right)\Delta x_j$ for the summands can be set to a desired value by a proper choice of the start and of the end point for each scale.

A *product* of functions can also be computed with a Type 1 nomogram. For example, consider again the equation $F = v_3 - v_1 v_2 = 0$ (see Sect. 2.1), from which one has $v_3 = v_1 v_2$ and then $\log(v_3) = \log(v_1) + \log(v_2)$, after taking the logarithm of both sides. This is a special case of Eq. (5), where all three g_j's are logarithmic functions.

As an example, in Fig. 4 we show a nomogram that we developed to compute the *logarithmic decrement* δ_n for a one-Degree-of-Freedom (1-DoF) harmonic oscillator, namely a system with a mass m (translating along a line) connected to a fixed frame through a spring of stiffness k and a viscous damper of coefficient c, with the spring and the damper acting in parallel. The logarithmic decrement is a classical topic in Mechanics of Vibrations and is commonly presented in undergraduate courses. From the definition of δ_n and known results on free vibrations of such systems, one finds

$$\delta_n = \log\left(\frac{x_1}{x_{n+1}}\right) = \frac{2\pi n\zeta}{\sqrt{1-\zeta^2}} \tag{6}$$

from which one has

$$\log\left(\delta_n\right) = \log(2\pi) + \log(n) + \log\left(\frac{\zeta}{\sqrt{1-\zeta^2}}\right) \tag{7}$$

Adding $\log(2\pi)$ to the logarithms of the input values in Eq. (7) is "embedded" in the way the scales have been drawn in Fig. 4, which is possible since $\log(2\pi)$ is a constant value, and does not complicate the nomogram. An isopleth has been added to show how a computation is performed[4]: for $\zeta = 0.4$ and $n = 3$, one has $\delta_n = 8.23$, which is found by drawing a straight line l over the points Z and N in Fig. 4 and finding the intersection D of l with the scale for δ_n. In a practical application, one generally finds δ_n by directly measuring the amplitudes of vibration x_1 and x_{n+1} at two time instants which are n oscillations apart, then applying the definition on the left-hand side in Eq. (6); the goal is then to derive the damping ratio ζ, which is otherwise difficult to measure. Notice that, while inverting Eq. (6) analytically to obtain ζ as a function of δ_n may be not immediate for a student, solving the inverse problem with the nomogram is just as easy as solving the original direct problem of computing δ_n from ζ.

To draw the nomogram in Fig. 4, we simply define three "blocks" in pyNomo, one for each scale. Each block defines the corresponding parameters, such as the maximum and minimum values, the labels and the function f_j used to draw the scale. A final block, linked to the previous ones for the scales, defines the type of nomogram to draw and (if required) the values to be used for the isopleths (Mottola, 2022).

The same equation can be represented in nomographic form in different ways. For example, another possible representation of a product of two variables $v_3 = v_1 v_2$ is given by an "N" (also called "Z") type nomogram, which is classified as Type 2 in Boulet et al. (2020): see for example Fig. 1c and d. Unlike a Type 1 nomogram, this latter design requires only one logarithmic scale (see again Fig. 1d). Let us consider three scales for the variables v_i, each starting at point $P_{jS} = (x_{jS}, y_{jS})$: this point corresponds to $g_j(v_j) = 0$. The direction of each scale is defined by vector $\left(\Delta x_j, \Delta y_j\right)$, which we assume to have unit magnitude, for simplicity. Equation (4) becomes

$$\begin{cases} f_{jx}(v_j) = x_{jS} + \Delta x_j g_j(v_j) \\ f_{jy}(v_j) = y_{jS} + \Delta y_j g_j(v_j) \end{cases} \quad \text{with} \quad g_j(v_{jS}) = 0 \quad \text{and} \quad \sqrt{\Delta x_j^2 + \Delta y_j^2} = 1 \tag{8}$$

while Eq. (3) in this case writes as

$$\begin{vmatrix} x_{1S} + \Delta x_1 g_1(v_1) & y_{1S} + \Delta y_1 g_1(v_1) & 1 \\ x_{2S} + \Delta x_2 g_2(v_2) & y_{2S} + \Delta y_2 g_2(v_2) & 1 \\ x_{3S} + \Delta x_3 g_3(v_3) & y_{3S} + \Delta y_3 g_3(v_3) & 1 \end{vmatrix} = 0 \tag{9}$$

If the scale for variable v_2 passes through P_{1S} and P_{3S}, and if the scales for v_1 and v_3 are parallel, it can be shown that linear scales can be set for v_1 and v_3, such that $g_1(v_1)$ and $g_3(v_3)$ are linear functions and that it holds $v_3 = v_1 v_2$. Since the only nonlinear scale is the one for v_2, the resulting nomogram is simpler to draw and, in some cases, more compact than the equivalent Type 1 nomogram for the same equation (obtained by using logarithmic scales, as previously explained). As an example, we have drawn another tool for computing the logarithmic decrement δ_n, but in this case by a Type 2 nomogram: the result is shown in Fig. 5. The fact that two of the scales are linear, while the one for ζ is only slightly deviating from linearity, arguably makes the resulting nomogram easier to read than the one in

[4] No units of measurement are reported here, since all parameters n, ζ and δ_n involved are dimensionless.

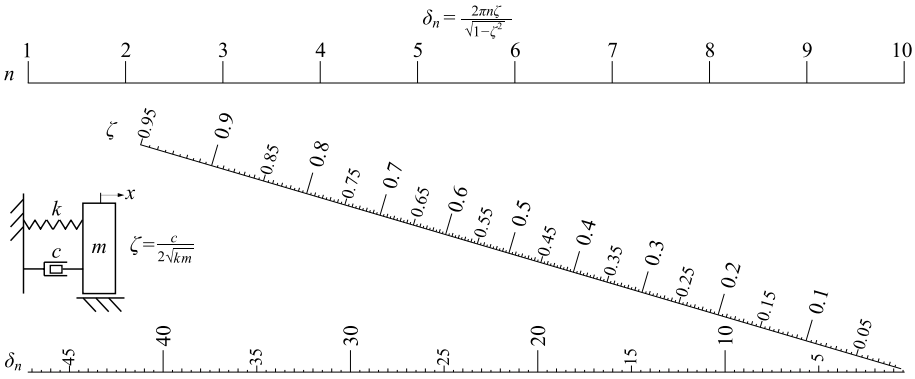

Fig. 5 Again on the logarithmic decrement δ_n, this time using a Type 2 nomogram (compare with Fig. 4)

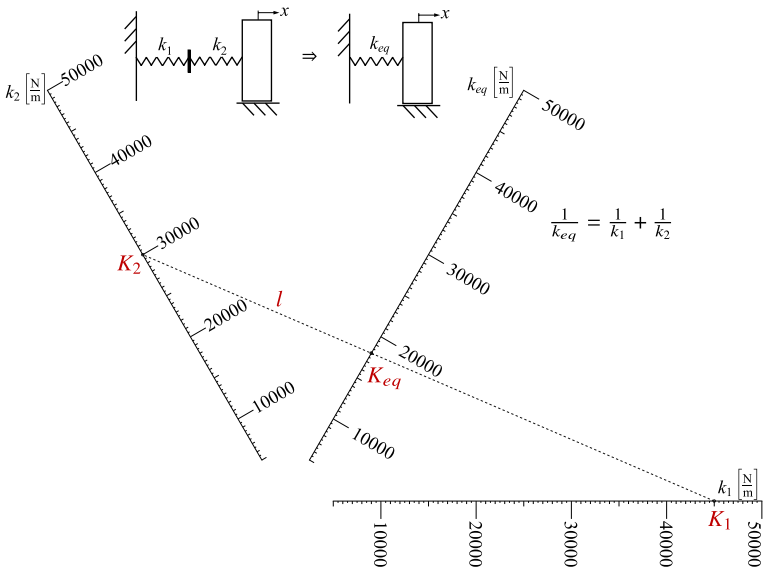

Fig. 6 Nomogram for the stiffness k_{eq} of a spring, equivalent to two springs in series having stiffnesses k_1 and k_2, respectively. Here, all three scales have the same units of measurement and the same unit length

Fig. 4; notice that this nomogram also allows us to display a longer range for the scale corresponding to the variable ζ.

Yet another design is the "concurrent scale" (or "angle") nomogram: an example is shown in Fig. 6. This kind of nomogram, classified as Type 7 in Boulet et al. (2020), is defined by three scales passing through a common point, which for simplicity is taken at the origin of all three scales: therefore, at point $P_{1S} = P_{2S} = P_{3S}$ it holds $g_1 = g_2 = g_3 = 0$. The origin O of the coordinate frame is also set at the same point. Having defined the angle α_j of the j-th scale with respect to the x-axis, one has

$$\frac{\sin\left(\alpha_3 - \alpha_2\right)}{g_1(v_1)} + \frac{\sin\left(\alpha_1 - \alpha_3\right)}{g_2(v_2)} + \frac{\sin\left(\alpha_2 - \alpha_1\right)}{g_3(v_3)} = 0 \tag{10}$$

One application for this kind of nomogram that is of interest for Mechanics of Machines is computing the equivalent total stiffness of a system of two linear springs attached in series, having stiffnesses k_1 and k_2, respectively. It can be shown that the resulting system is statically equivalent to a single spring of stiffness k_{eq}, having

$$\frac{1}{k_{eq}} = \frac{1}{k_1} + \frac{1}{k_2} \tag{11}$$

This equation can be directly implemented in a Type 7 nomogram: see Fig. 6. Here, the isopleth l has been drawn for an example calculation with $k_1 = 45000$ N m^{-1} and $k_2 = 30000$ N m^{-1}, corresponding to points K_1 and K_2, respectively; the resulting equivalent stiffness $k_{eq} = 18000$ N m^{-1} is found at point K_{eq}, on the intersection of l with the third scale. Notice that unrealistic cases with either $k_1 = 0$ or $k_2 = 0$ are excluded by design: it is thus impossible to obtain incorrect results due to misreading the input. The angles α_j can be chosen according to our preference; if $\alpha_3 - \alpha_2 = \alpha_2 - \alpha_1 = 60°$, as in Fig. 6, all scales conveniently have the same unit length.

Finally, we discuss the Type 4 (or "proportion") nomogram (Boulet et al., 2020). A remarkable feature of this design is that it allows us to solve equations in *four* variables, instead of *three* as in the other types. Therefore, the corresponding equation cannot be written in the form shown in Eq. (3); nevertheless, this is still an alignment nomogram and its equation can be written in determinant form, for example as

$$\begin{vmatrix} 1 & 0 & 0 \\ 0 & f_1(v_1) & f_2(v_2) \\ 0 & f_3(v_3) & f_4(v_4) \end{vmatrix} = 0 \tag{12}$$

which is equivalent to

$$\frac{f_1(v_1)}{f_2(v_2)} = \frac{f_3(v_3)}{f_4(v_4)} \tag{13}$$

Figure 7 shows how such a nomogram is used: suppose that the v_2 (corresponding to the scale on the right) is the unknown which we seek as the output of the graphical computation, while v_1, v_3 and v_4 are known input parameters. We then draw a line through the points for v_4 and v_3 (corresponding to the top and the bottom scale, respectively), which intersects the auxiliary line at 45° with respect to the horizontal at a point A: we then draw a second line through A and the point for v_1, which intersects the scale on the right in a point corresponding to the value for v_2 which solves Eq. (13).

While Type 4 nomograms are more flexible, in our experience a significant drawback is in that they make it difficult for the designer to properly choose the ranges for each scale. In general, the choice of the minimum and maximum values to display in each scale significantly affects the readability and usefulness of the nomogram: in a practical case, realistic values are suggested by experience, but if the resulting scale is too long or too short it becomes difficult to find the desired value. In a Type 4 nomogram, this is complicated by the fact that the scales are interdependent.

As an example, we refer the reader to Fig. 7, a nomogram which we designed to analyze the Hertzian contact stresses between two elastic curved bodies: this is another common topic in Applied Mechanics courses which frequently leads to rather complex equations which lack an immediate physical interpretation. Considering in particular two elastic spheres composed of the same material, pushed against each other by a contact force P

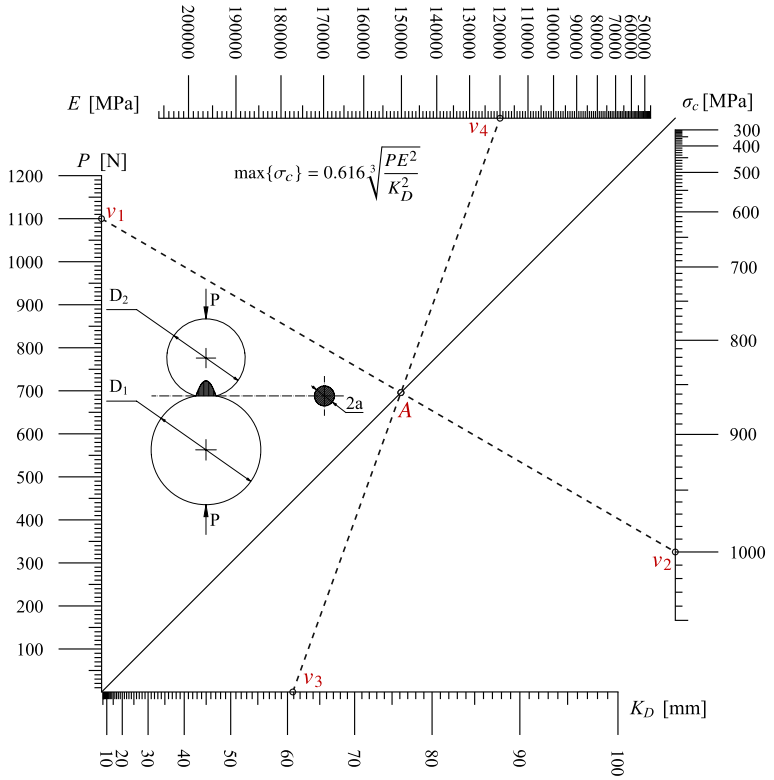

Fig. 7 A Type 4 nomogram for computing the maximum Hertzian compressive stress between two balls, respectively having diameters D_1 and D_2, kept in contact by a force P; the contact area is a circle of diameter $2a$. We assume that the material is the same for both spheres and that it has a linear elastic behavior, defined by the constant parameters E (the Young's modulus) and $\nu = 0.3$ (the Poisson's ratio)

along the common axis between the centers of the spheres, the maximum compressive stress σ_c in the zone of contact is (Young and Budynas, 2002)

$$\max\{\sigma_c\} = 0.616\sqrt[3]{\frac{PE^2}{K_D^2}} \tag{14}$$

in which E is the Young's modulus of elasticity for the material, which is the same for both spheres; it is assumed that this material has ideal linear elastic behavior and that its Poisson's ratio is $\nu = 0.3$, which is a common value for both steel and aluminum alloys. The parameter K_D, which has units of length, is given by (Young and Budynas, 2002)

$$\frac{1}{K_D} = \frac{1}{D_1} + \frac{1}{D_2} \tag{15}$$

where D_1 and D_2 are the diameters of the two spheres, respectively. Notice that this parameter could be computed with another nomogram, for instance with a Type 7 design: comparing Eq. (15) with Eq. (11), the similarities are apparent.

The resulting nomogram for Eq. (14) is shown in Fig. 7; a similar nomogram could be drawn to compute the radius a of the contact area, which is a circle in this case. Limit cases, such as the contact between a sphere and a plane (when one of the diameters D_i goes to infinity) can be still be analyzed through the same nomograms.

Considering more general cases, such as the spheres being composed of different materials, introduces other variables: therefore, one needs to combine multiple nomograms together, to compute intermediate terms. This is in fact one of the strongest advantages of alignment nomograms over, for example, lookup graphs: a few examples of more complex combined nomograms are presented in Sect. 4. The possibility of combining nomograms is already provided in the pyNomo library, which greatly simplifies the design. While nomograms provide an aesthetically pleasing, easy to read graphical tool, one of their drawbacks is that introducing more and more variables in an equation, to consider more general cases, quickly leads to unwieldy designs that are difficult to read and which must be printed in very large format for readability. In our experience, equations in more than eight independent variables become impractically complex for nomography: unless some special cases of interest can be defined, with some variables having fixed values (which reduces the number of scales in the design), other computing methods, such as software tools, should be used instead.

We conclude our discussion by noting that there are several designs in the literature that extend the concepts above and thus cannot be easily categorized. For instance, some nomograms use circular scales (such as the Smith chart), while others use more complex curves such as the *folium* of Descartes; with this design, some nomograms were devised for the product of two variables, where all three scales coincide (Doerfler, 2009; Evesham, 1986). When curved scales are used, more than one intersection point may be found, corresponding to different solutions (for nonlinear equations).

Equation (3) can also be generalized to contain up to six variables, as

$$\begin{vmatrix} f_{1x}(u_1,\, v_1)\; f_{1y}(u_1,\, v_1)\; f_{1z}(u_1,\, v_1) \\ f_{2x}(u_2,\, v_2)\; f_{2y}(u_2,\, v_2)\; f_{2z}(u_2,\, v_2) \\ f_{3x}(u_3,\, v_3)\; f_{3y}(u_3,\, v_3)\; f_{3z}(u_3,\, v_3) \end{vmatrix} = 0 \tag{16}$$

which is defined as a Type 9 nomogram in Boulet et al. (2020) and Martínez-Pagán and Roschier (2022). In this case, each scale is replaced by a graduated grid in the two variables u_j and v_j, which define a point on the grid; the resulting nomogram is still defined by the alignment of three points (one for each grid). While more flexible, these nomograms easily lead to cluttered and hard to read designs, which goes against the spirit of having a readable tool enhancing the visualization of the results.

4 Applications of Nomography

To illustrate concrete applications of nomography in the analysis of machines and mechanisms, we present a few example designs of more complex nomograms, devised to solve some practical problems. The first one, shown in Fig. 8, has been developed for the kinematic analysis of a spatial mechanism. This design has been inspired by a collaboration with a company working on variable-displacement axial piston pumps; a swashplate can be rotated by an angle α to control the displacement. The company reported a need to compute the pump displacement from direct measurements on its components: this is useful when working on a shop floor, as the pump data (such as the serial number and product

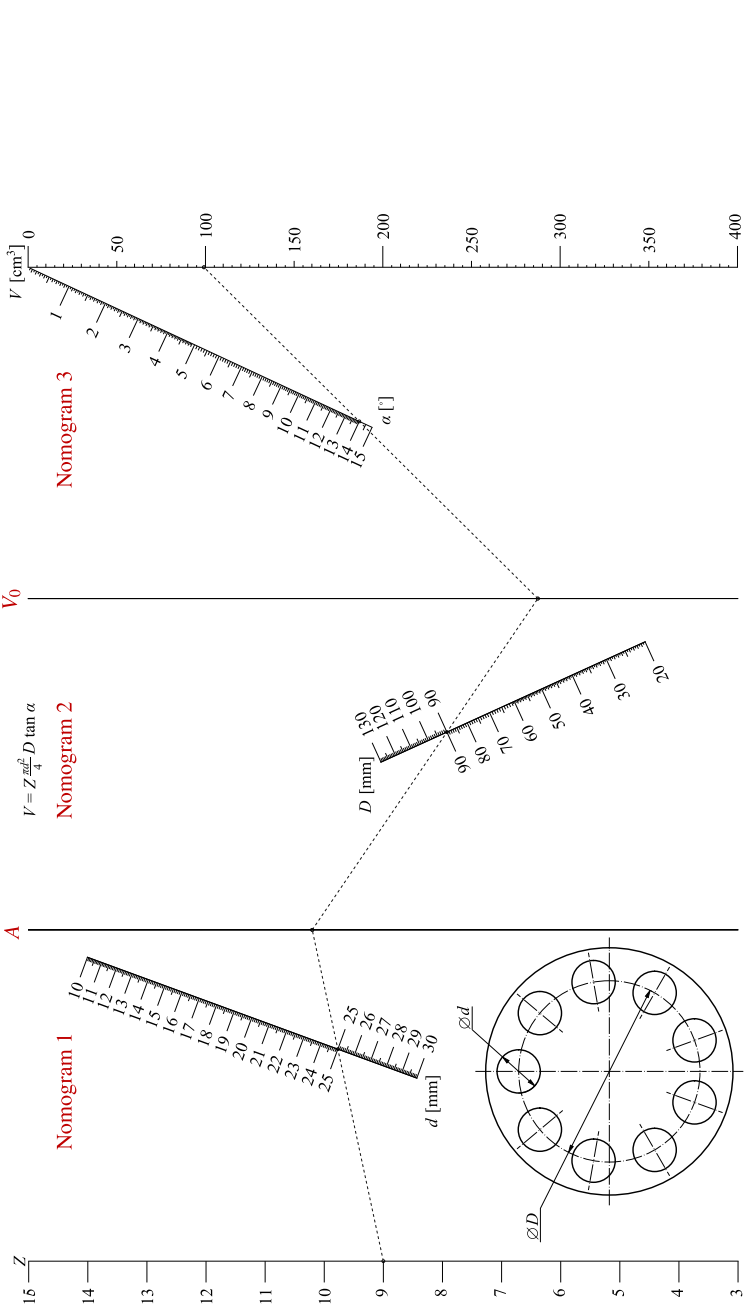

Fig. 8 A combined nomogram (composed of three "intermediate" Type 2 nomograms) for calculating the displacement of a volumetric axial piston pump with a swashplate

specification) may not always be directly available. The displacement V can then be computed from easily measured quantities, as

$$V = \frac{\pi d^2}{4} ZD \tan(\alpha) \tag{17}$$

where d is the piston diameter, Z their number and α the swashplate inclination. The axes of translation of the pistons all lie on a (virtual) cylindrical surface of diameter D. Clearly, Eq. (17) can be implemented in any computation software, for instance as a spreadsheet. However, operating a digital device when disassembling a pump (which is generally filled with lubricant) for maintenance operations is clearly inconvenient. Moreover, there is a significant risk of operator errors due to incorrect data entry.

Nomograms are an interesting option for this task. However, Eq. (17) contains five variables; thus, it cannot be directly expressed as a nomogram of one of the types presented previously. We then divide the nomogram design in three parts, as follows.

1. We create a nomogram to compute $A = \frac{\pi d^2}{4} Z$: this corresponds to the global cross-sectional area of the pistons. This is achieved through a simple Type 2 nomogram with three variables, as described in Subsect. 3.1, namely $v_1 = d^2$, $v_2 = Z$ and $v_3 = A\frac{4}{\pi}$: the product $v_3 = v_1 v_2$ is on the auxiliary scale denoted by A in Fig. 8.
2. The result from the previous nomogram is used in the second step, by joining the two nomograms at the scale A; this second nomogram computes $V_0 = DA$. Again, having a product of two variables, a Type 2 nomogram is used here.
3. Finally, a third nomogram is introduced, joined with the previous one at the scale for V_0. This gives $V = V_0 \tan(\alpha)$, namely the displacement for each pump rotation.

The final result is shown in Fig. 8; here, the two vertical scales in the middle correspond to variables A and V_0, respectively. The numerical values of these intermediate quantities are not required by the user; thus, no ticks are displayed, to avoid cluttering the graph. The isopleth on the graph shows an example calculation for a realistic pump design; on one corner of the nomogram, a sectional view of the central cylinder block of the pump is shown for reference, to clarify the definitions of diameters D and d.

This nomogram can be printed on laminated paper, to protect it from oil spills, and introduced in shop-floor practice for quick computations. The isopleths at each step can be found with a rigid element having a straight-line segment of sufficient length.

We also suggest applications for educational purposes. As noted in Doerfler (2009), Douglas and Danciu (2020), Kattan and Marasco (2010), Martínez-Pagán and Roschier (2022), Tournès (2003), nomograms allow the user to easily understand the properties of equations with complex algebraic expressions; also, nomography is a graphical approach that makes it unlikely to misinterpret inputs or results. Besides nomograms, other graphical methods, such as those used for planar mechanism kinematics and statics, are currently taught in mechanical engineering courses. While these methods could be replaced with purely analytical approaches, they are still used due to their pedagogical value. We thus expect nomograms to easily fit in existing courses; in particular, nomography extends graphical approaches for computation to any equation that can be written in determinant form as in Eq. (3). Some personal experiences on nomograms for math education in high schools were reported in Tournès (2018); a test on their usefulness for university-level education would then be worthwhile to understand their strengths and limitations. We also believe that mentioning examples of nomograms, together with their uses and applications,

within a course in Mechanics of Machines, could also enhance interest among students in historical methods for engineering analysis and in its broader historical development.

In a future development, we suggest that a few nomograms could be used in a course alongside the equations for which they were defined. This would be especially impactful if said equations are defined by complex formulae (but with relatively few variables) and depend on non-integer coefficients: in these cases, using a nomogram can be quicker (and less prone to errors) than reporting the equations on a handheld calculator. A simple experiment would be to provide nomograms as a solution tool during open-book exams or for home exercises: at the end, students would be asked to complete a questionnaire on which computing tool they used. While this would require devoting a few moments during the course to explaining how nomograms are used (since students can no longer be expected to be already familiar with them), results on the share of students who spontaneously adopted them would provide an important indicator on whether nomograms can still be useful as a teaching tool.

For the reasons outlined above, we devised a few nomograms on topics frequently discussed during a course on Mechanics of Vibrations. The first one is shown in Fig. 9 and it has been developed to compute the first resonance frequency f of an inextensible taut string. This is usually the first example presented to the students of a *continuous* vibrating system, namely an element which has infinitely many DoFs and thus an infinite number of resonance frequencies. Under the usual assumption of small vibrations with respect to the equilibrium configuration (namely, with the string on a straight line segment), the first natural frequency is (Young and Budynas, 2002)

$$f = \frac{1}{2l}\sqrt{\frac{T}{\rho}} \tag{18}$$

where l is the length of the string from one fixed attachment point to the other, T is the string tension and ρ its linear density; it is assumed that the string has uniform section and that it can only withstand tensile forces (that is, it has zero flexural stiffness).

As shown in Fig. 9, since Eq. (18) contains four variables, the nomogram can be obtained by combining two simpler Type 2 nomograms. The final result, namely the vibration frequency, is shown on the rightmost scale. An interesting feature of nomograms is that two different scales can be accommodated along the same line, for instance to convert results between different units of measurement: indeed, the frequency in Fig. 9 is reported both in hertz and with the corresponding musical note (expressed in the international pitch notation). This increases the educational value of the nomogram in the classroom, as it allows to directly link the numerical result to something that the students (at least, those with some musical training) may understand more immediately; this link is otherwise far from obvious when looking at Eq. (18). This nomogram has indeed been developed by considering a musical instrument (the classical guitar) as a reference: meaningful values, obtained from producers' catalogs, were defined for the string density, taking into account the different materials that can be used[5]. The corresponding values are reported on the scale for ρ. Similarly, the range for the length L and for the tension T has been derived from manufacturers' websites. Notice that the resulting range for f is somewhat unrealistic, as the maximum frequency D_5 obtained is too high for a classical guitar; this is due to a

[5] Usually, strings either made of Nylon or of steel-coated Nylon are used, respectively for the higher and the lower pitches.

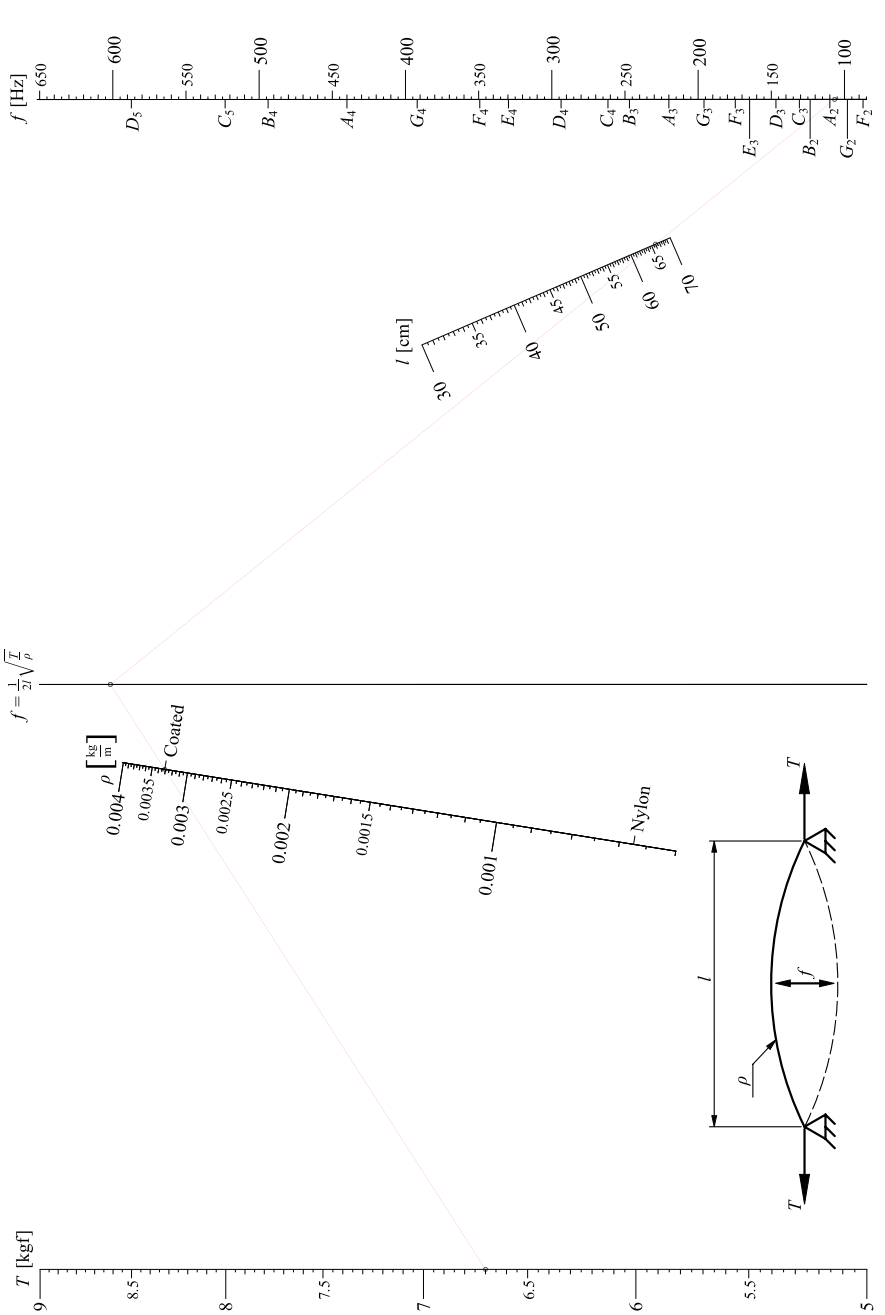

Fig. 9 A combined nomogram (composed of two Type 2 nomograms) for calculating the first natural vibration frequency of a guitar string and the corresponding note

design choice, in which we consider all possible values for each of the input scales and compute the corresponding possible range for f (even considering the "extreme" case of maximum T and minimum l and ρ). This can be useful in a classroom, to explore the full set of possibilities for a theoretical formula such as Eq. (18); in a practical case, one may otherwise choose to artificially restrict some ranges according to data or personal experience, to exclude unrealistic values. An interesting exercise that could then be proposed to students is to consider a real guitar cord, with assigned values of ρ and l, and explore the full range of notes that can be achieved by changing the tension T, to obtain a deeper understanding of the influence of the input values on the final results.

Another nomogram that we developed for educational purposes is presented in Fig. 10. Let us consider again the 1-DoF damped harmonic oscillator introduced in Sect. 3.1, for which we aim to find the *critical damping ratio*. This is the value c_{cr} which determines the behavior of the system under free vibrations: in particular, if the actual damping coefficient c is lower than c_{cr} there will be a damped periodic motion, otherwise the motion will be aperiodic and exponentially converging to the equilibrium position without oscillations. For a system having mass m and stiffness k, it holds

$$c_{cr} = 2\sqrt{km} \tag{19}$$

To provide a concrete example to the students, we assume that the compliance of the system is given by a rubber spring having cylindrical shape, as shown in Fig. 10; the spring design is defined by its height h, diameter d and by the Young's modulus E of the rubber. The stiffness is then found as (Young and Budynas, 2002)

$$k = \frac{\pi d^2 E}{4h} \tag{20}$$

Finally, we assume for simplicity a linear viscous behavior to model damping effects: thus, the damping force is given by $F_d = c\dot{x}$, where x is the displacement from the equilibrium position of the mass m and $\dot{x}$ is its velocity[6].

The nomogram for computing c_{cr} in Fig. 10 is obtained by combining two nomograms, one (on the left) implementing Eq. (20) for the stiffness k, and the other (on the right) for solving Eq. (19) from the known values of k and m. In the first nomogram, two scales are reported to define the elastic properties of the rubber: indeed, while most manuals on Machine Design report Eq. (20) as a function of the elastic modulus, it is common in engineering practice to measure the hardness of rubber materials in Shore degrees (indicated as °Sh). These two parameters, however, are generally not independent, and several functions have been proposed for correlating them: here we take the one advanced in Gent (1958), which is expressed as

$$E = \frac{0.0981(56 + 7.66S)}{0.137505(254 - 2.54S)} \tag{21}$$

in which E is expressed in MPa and S is the rubber hardness (using a durometer according to the standard ASTM D2240 Type A). In a sense, this doubly-graduated scale can be seen as another nomogram, specifically an example of a Type 8 nomogram according to Boulet

[6] In a practical case, the viscous model is not strictly valid, as the internal hysteresis of the rubber should be taken into account; however, in an educational setting this would distract from the example and complicate the design of the nomogram.

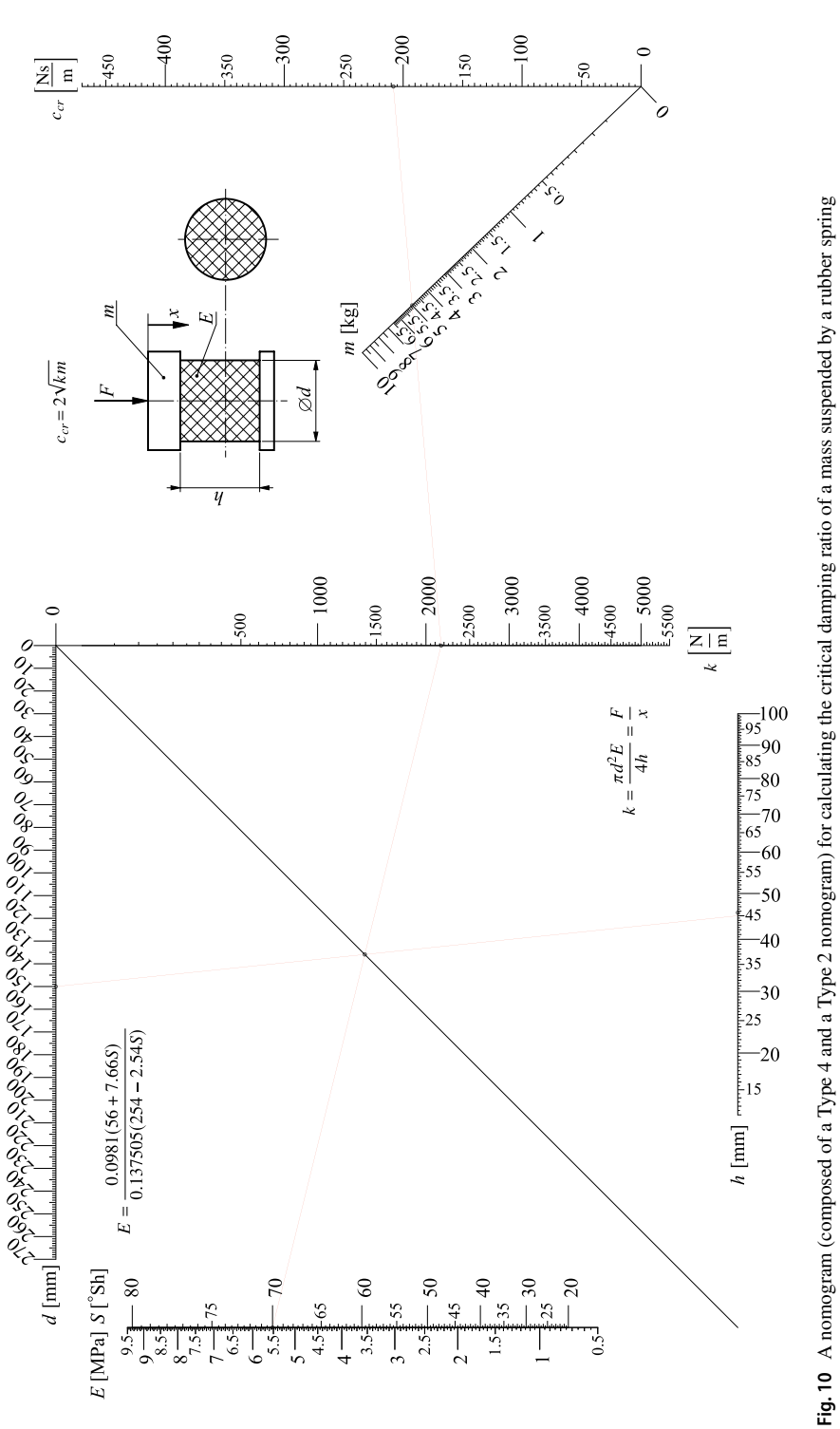

Fig. 10 A nomogram (composed of a Type 4 and a Type 2 nomogram) for calculating the critical damping ratio of a mass suspended by a rubber spring

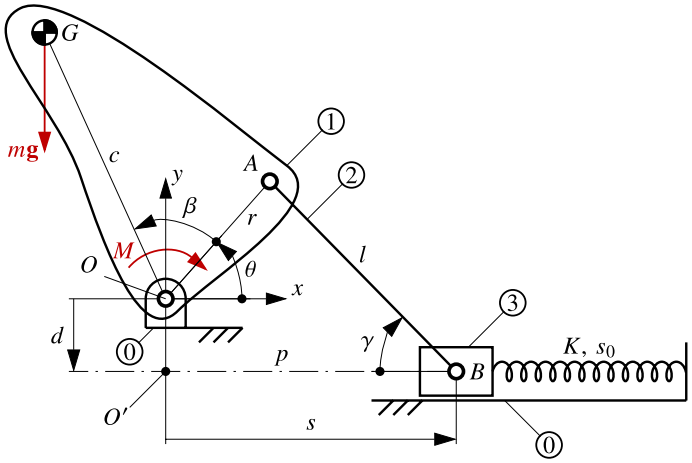

Fig. 11 Schematic of a planar slider-crank linkage with a spring between links 0 and 3 for static balancing

et al. (2020) and Martínez-Pagán and Roschier (2022). This is a simpler nomogram with a single scale, graduated on both sides: this design allows us to compute functions in one variable $v_2 = f(v_1)$, by reporting the values for v_1 on one side of the scale and those for v_2 on the other side. The conversion in Eq. (21) is defined by a complex equation depending on numerical coefficients: it would then be easy to make a typing mistake when using a handheld calculator or reporting the formula in a spreadsheet. Using the nomogram in Fig. 10, on the other hand, is straightforward.

In this nomogram, as in Fig. 9, an isopleth has been drawn (with a thin red line) to illustrate an example calculation. A student may then explore the design alternatives and their effect on the final results, for instance by verifying how the coefficient c_{cr} changes depending on the type of rubber used for the spring (all other parameters being equal). The nomogram could also report on the leftmost scale some reference values of Shore hardness for common industrial rubbers, providing also practical guidance in the evaluation of realistic values for an example rubber which is yet to be tested.

As a last example, we present a nomogram that can be used in a design or research setting. An active topic of study in Machine Design is devising *statically-balanced mechanisms*, namely mechanical systems which are in a constant state of neutral static equilibrium under the effect of gravity. These devices are of practical importance in robotics (Mottola et al., 2022), where they can be used to compensate or at least reduce the torque at the motors due to the gravitational force, or in handheld tools such as lamps and desks, to reduce the effort required by the user to move the tool at the desired position. These mechanisms generally employ either counterweights or springs to balance the effects of the own weight of their links; the goal is to obtain a system which can move while maintaining constant (or almost constant) total energy

$$V_t = V_g + V_e \tag{22}$$

due to all conservative forces: these are introduced by gravity, whose contributions are grouped in the term V_g, and by the elastic elements, corresponding to term V_e. In the following, as it is commonly done in this area of research, we assume that all forces are in fact conservative: therefore, for example, we disregard frictional effects.

Let us now consider a 1-DoF system, such as the slider-crank planar mechanism shown in Fig. 11. Here, the crank 1 revolves around the fixed frame 0 around a revolute (R) joint in point O, and is connected to the coupler 2 with an R joint in A; finally, the slider 3 is connected with another R joint in point B to the coupler, and translates along axis p of a prismatic (P) joint with respect to the frame. A reference point O' is defined at the projection of O along p. All links are assumed to be perfectly rigid; the motion takes place in the vertical plane under the effect of gravity. The kinematic equations are found from the loop-closure constraint on $OABO'$: considering its components along the x and y axes (which define a coordinate system with origin in O), we obtain

$$\begin{cases} s = l\cos(\gamma) + r\cos(\theta) \\ d = l\sin(\gamma) - r\sin(\theta) \end{cases} \tag{23}$$

with $s = \overline{O'B}$, $l = \overline{BA}$, $r = \overline{AO}$, and $d = \overline{OO'}$; angle θ is defined between segment OA and the horizontal x axis, while $\gamma = \widehat{O'BA}$. Without loss of generality, we consider units of length such that $l = 1$. From Eq. (23), with algebraic manipulation one obtains

$$s = r\cos(\theta) + \sqrt{1 - [d + r\sin(\theta)]^2} = s(\theta) \tag{24}$$

The crank has its center of mass (CoM) in G, at distance c from O. The crank weight is $m\mathbf{g}$, where $\mathbf{g} = \left[0, -g\right]^T$ is the acceleration vector (with $g = 9.80665\ \mathrm{m/s^2}$); the masses of the other links are disregarded. The term V_g due to gravity in Eq. (22) is then

$$V_g = gc\sin(\theta + \beta) \tag{25}$$

where $\beta = \widehat{AOG}$; the mass m is assumed to be 1 in a suitable system of units.

An ideal (linear) spring of stiffness K is attached between the slider 3 and the fixed frame 0, to balance the weight of the crank. This spring stretches along axis p as the slider moves, and is at rest when $s = s_0$. Thus, the elastic potential V_e is

$$V_e = \frac{1}{2}K\left(s - s_0\right)^2 \tag{26}$$

We assume that the mechanism geometry, defined by r, c, β and d, is given and cannot be changed. We then seek the "best" spring, defined by parameters K and s_0, which minimizes the residual torque M that must be applied at O to balance the mechanism under static conditions (disregarding inertial effects): we then have

$$M(\theta) = \frac{d}{d\theta}V_t(\theta) = \frac{dV_g}{d\theta} + \frac{dV_e}{d\theta} = \underbrace{gc\cos(\theta + \beta)}_{M_g(\theta)} + \underbrace{\frac{1}{2}K\frac{d}{d\theta}\left[s(\theta) - s_0\right]^2}_{M_e(\theta)} \tag{27}$$

in which we have made explicit the dependence of the energy V_t from Eq. (22) and of the torque M on the angle θ, which defines the configuration of the mechanism. If $V_t(\theta)$ is a constant, then $M(\theta)$ is always zero and the mechanism is in static equilibrium for a continuous range of configurations. Notice that, while the weight acting on the crank is constant, the corresponding torque $M_g(\theta)$ at O due to said weight is instead a nonlinear function of the position, which complicates the balancing.

In a practical case, however, perfect balancing may not be necessary: if the residual torque M is sufficiently small over the required range of motion $\theta \in \left[\theta_{min}, \theta_{max}\right]$, it can be acceptable to leave the mechanism partly unbalanced (Radaelli et al., 2011), as frictional

effects generally help in maintaining static equilibrium. Otherwise, more complex balancing mechanisms may be added, such as cam-follower systems (Hain, 1961; Hilpert, 1968): the slider-crank mechanism can then balance most of the unbalance torque $M_g(\theta)$, while a cam-based linkage, which is usually more delicate, compensates the remaining smaller term while having to withstand smaller forces.

An application of the mechanism shown in Fig. 11 can be derived by fixing the crank 1 on a component which is to be balanced: G is then the global CoM of the components moving together, and m is the total mass of the crank and of the component to which it is attached. This design could be usefully applied, in robot arms or hand-operated devices: for example, similar concepts are known from the patent literature for hinges to be applied on furniture doors, to prevent them from slamming down.

Equation (27) could be studied analytically, in order to find a choice of K and s_0 that makes the right-hand term identically zero for all θ; however, we are not aware of previous exact results in this area. Here, instead, we suggest a mixed numerical-graphical method, whose application to statically-balanced mechanisms is novel, to the best of our knowledge. Our approach is as follows: we consider a set of possible mechanisms having the same schematic (Fig. 11), with each mechanism being defined by a combination of r, c, β and d (whose values are within given ranges of interest for the geometric parameters), and a range of rotation angles $\theta \in \left[\theta_{min}, \theta_{max}\right] = \Theta$. For each element in the set, we solve the following optimization problem:

$$\min_{K>0,\, s_0 \in \mathbb{R}} \left(\max_{\theta \in \Theta} M(\theta) \right) \tag{28}$$

and store the values of K_{opt} and $s_{0,opt}$ thus obtained. Then, we seek an interpolation function which approximates the optimal values of K and s_0 from the corresponding values of the geometric parameters: while in general this function will not provide the exact optimum, the error can be made reasonably small if the interpolating function is properly chosen. The approximation is also less of an issue here since even the optimal values do not, in general, provide an exact balancing. These approximate functions $K_{opt} = f_K(r, c, \beta, d)$ and $s_{0,opt} = f_s(r, c, \beta, d)$ can provide useful guidance to the designer, who will not have to solve the optimization problem in Eq. (28), which is nonlinear (and thus in general quite complex). Being approximations of numerical data, the functions f_K and f_s are in general complex to write and compute and contain approximate coefficients; thus, as seen for Eq. (21), which interpolates experimental data, a nomogram can speed up the computation and reduce the risk of errors.

The space of possible mechanisms is defined by four geometric parameters r, c, β and d, which leads to a rather complex nomogram. For simplicity, we now consider the important special case in which the offset d is zero, namely the in-line slider-crank. To further simplify the analysis, we then consider two extreme positions of the linkage, at $\theta + \beta = \frac{\pi}{2}$ and at $\theta + \beta = -\frac{\pi}{2}$. From Eq. (27), it is apparent that at these positions the torque $M_g(\theta)$ due to the gravitational term is zero. If we require having exact static equilibrium at least at these two positions, with no residual unbalance torque M, it follows that it must hold $M_e(\theta) = 0$, too; expanding Eq. (27), we find

$$M_e(\theta) = \frac{1}{2} K \frac{d}{d\theta} \left[s(\theta) - s_0 \right]^2 = \frac{1}{2} K \cdot 2 \left[s(\theta) - s_0 \right] \cdot \frac{d}{d\theta} s(\theta) \tag{29}$$

(recall that s_0 is a constant). In Eq. (29), K cannot be zero, as that would be equivalent to having no balancing spring; therefore, it must either be $s(\theta) = s_0$ or $\frac{d}{d\theta} s(\theta) = 0$. Since

$s(\theta) = s_0$ cannot hold at both positions, we require the derivative of $s(\theta)$ to be zero: this condition defines the two limit positions of the mechanism, at the opposite extremes of the stroke. From this condition and simple geometry, it is easy to show that it must be either $\beta = \frac{\pi}{2}$ or $\beta = -\frac{\pi}{2}$; we then take the first condition in our design.

Having set $d = 0$ and $\beta = \frac{\pi}{2}$, we launched a numerical simulation, in which we explored all mechanisms in the ranges[7] $c \in [2, 18]$ and $r \in [0.05, 0.35]$. After discretizing the ranges of input geometric parameters, we then solved Eq. (28) for each mechanism and interpolated the resulting optimum values of K and s_0 as functions of c and r. For simplicity, we used a Type 2 nomogram such as the one in Fig. 5, which computes the product of two functions: we thus needed to interpolate the results as $K_{opt} = f_K(r, c) = f_{K1}(r) f_{K2}(c)$ and $s_{0,opt} = f_s(r, c) = f_{s1}(r) f_{s2}(c)$. As a compromise between accuracy and simplicity, we used 7^{th} order rational approximants for both functions f_K and f_s. The use of rational functions (expressed as a ratio of polynomials) to approximate a given function is well known and is already implemented in numerical subroutines. Moreover, rational functions can be used to approximate a large class of functions and are usually simple to compute with nomograms. All the optimization and interpolation problems were solved in MATLAB.

We thus found

$$K_{opt} = g \frac{-128c(4 + r^2)}{r(-512 + 64r^2 + 36r^4 + 5r^6)} \tag{30}$$

and

$$s_{0,opt} = \frac{1024 - 59.5r^4 - 6.94r^6}{124.7r^2 + 512.2} \tag{31}$$

The parameter c was found to have almost no influence on the optimal free length of the spring: thus, it does not appear in Eq. (31). The design in Fig. 12 is a combination of a Type 2 nomogram, to compute K_{opt} by implementing Eq. (30), and a Type 8 nomogram, to find $s_{0,opt}$ as a function in a single variable from Eq. (31).

The resulting mechanisms, while not perfectly balanced in general, are found to have very small residual unbalanced torques M: in the worst-case scenario among all mechanisms considered, the maximum value of M was reduced by 94.7% with respect to the corresponding maximum value without the balancing spring. While Eqs. (30) and (31) only provide approximations of the optimal design values, the errors with respect to the results from the optimization problem in Eq. (28) never exceed 0.1%.

A nomogram such as the one in Fig. 12 is thus found to be an effective design tool, which condensates a large mass of data in a simple schematic; it could then be applied by designers who need to apply the generic concept in Fig. 11 to several use cases, with no need to solve optimization problems (which usually require software packages that are vast and complex to use) nor to understand the finer details of the design equations.

[7] The units are not reported, as these values correspond to the adimensional ratios c/l and r/l; the length s_0 is also normalized with respect to l. K is normalized with respect to both l and the mass m (and thus has units of acceleration).

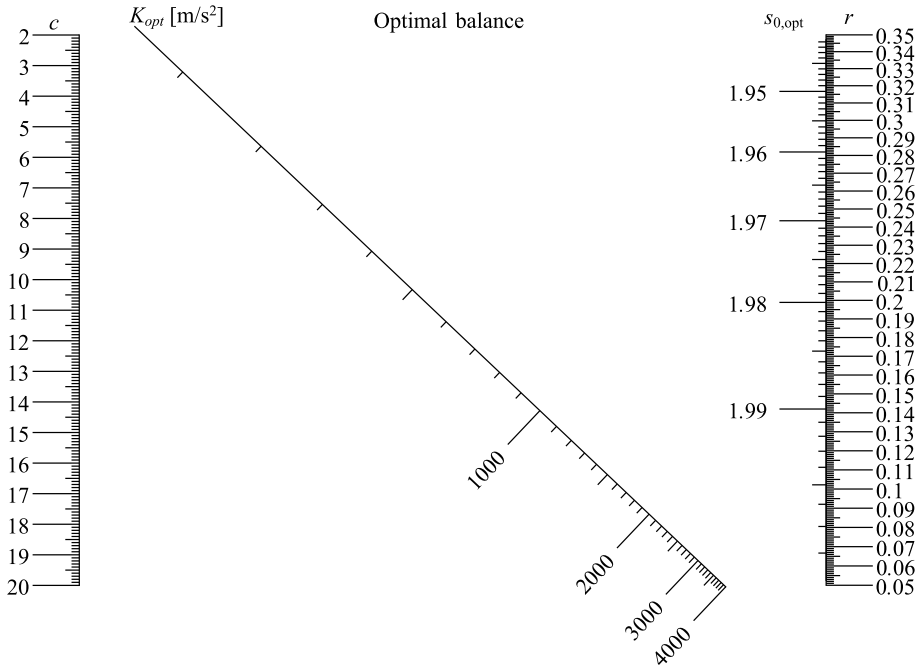

Fig. 12 A nomogram for generating optimally-balanced slider-crank linkages; see also Fig. 11

5 Conclusion and Future Work

In this paper, we present a short history of nomography, a graphical computing method which used to be a common tool for both scientists and engineers. We thus discuss the ideation and development of this concept, together with a selection of its applications (especially in mechanical engineering); we also present a few example nomograms, together with their mathematical properties. Finally, we show some nomograms that we developed especially for educational and design purposes. In our research, we used pyNomo, an open-source library (under GPL3 license) which greatly facilitates the work of the nomographer: we thus find that software, which cause the progressive decline of interest in nomograms, can help in bringing renewed interest in these tools.

In future work, we aim to propose nomograms in educational settings, for instance within a course in Mechanics of Machines: this way, we may appreciate their actual effectiveness for didactic purposes. Nomograms would be discussed in the classroom, by comparing them to the equations from which they were derived and with other graphical methods, for instance by introducing a brief seminar during the course. The perceived advantages and disadvantages of nomograms would be evaluated by proposing questionnaires to the students at the end of the course. The necessity of defining methods to scientifically evaluate the pedagogical impact can also provide an interesting opportunity for cross-sector collaborations with researchers in psychology and social sciences. We also aim to develop some new nomograms for more complicated topics, such as Assur groups or matrices for 3D rotations, which frequently cause difficulties for the students. It is hoped

that this work can also renew interest among researchers in the intriguing mathematical properties of nomograms.

Acknowledgements The authors thank the chair and the Scientific Committee of the "*7th International Symposium on History of Machines and Mechanisms (HMM 2021)*" for selecting our previous conference paper Mottola and Cocconcelli (2022) to be revised and extended for publication in the present special issue.

Declarations

Conflict of interest The authors declare no competing interests. The scripts generated during the current study are available in the "Nomograms-for-mechanical-engineering" repository, https://doi.org/10.5281/zenodo.7258700

References

Adams, D.P. (1950). An index of nomograms. The Technology Press of Massachusetts Institute of Technology.

Adams, D. P. (1960). Nomographic synthesis of generator linkages. *Journal of Engineering for Industry, 82*(1), 29–38. https://doi.org/10.1115/1.3662986.

Aleksandrov, I. K. (2011). Determining the limiting efficiency of a kinematic chain. *Russian Engineering Research, 31,* 539–540. https://doi.org/10.3103/S1068798X11060037.

Antuma, H. J. (1978). Triangular nomograms for symmetrical coupler curves. *Mechanism and Machine Theory, 13*(3), 251–268. https://doi.org/10.1016/0094-114X(78)90049-6.

Bagaria, W. J., Doerfler, R., & Roschier, L. (2017). Nomograms for the design of light weight hollow helical springs. *Proceedings of the Institution of Mechanical Engineers, Part C, 231*(23), 4388–4394. https://doi.org/10.1177/0954406216665416.

Bond, W. L. (1948). A simple procedure for the making of alignment charts. *Journal of Applied Physics, 19*(1), 83–86. https://doi.org/10.1063/1.1697877.

Boulet, D., Doerfler, R., Marasco, J. & Roschier, L. (2020). pyNomo documentation. http://lefakkomies.github.io/pynomo-doc/index.html

de Freitas Avelar, A. H., Roschier, L., Fernandes Soares, L., & Oliveira Ávila, P. H. S. (2021). Analytical solutions and computational nomograms for maximum pressure angle for cam mechanisms for full and half cycloidal and harmonic motion curves. *Journal of Mechanical and Engineering Science, 235*(15), 2725–2736. https://doi.org/10.1177/0954406220962823

d'Ocagne, M. (1899). Traité de nomographie. Paris: Gauthier-Villars.

Doerfler, R. (2009). On jargon–the lost art of nomography. *The UMAP Journal, 30*(4), 457–493.

Douglas, J., & Danciu, L. (2020). Nomogram to help explain probabilistic seismic hazard. *Journal of Seismology, 24,* 221–228. https://doi.org/10.1007/s10950-019-09885-4.

Éidinov, M. S., Nyrko, V. A., Éidinov, R. M., & Gashukov, V. S. (1976). Torsional vibrations of a system with Hooke's joint. *Soviet Applied Mechanics, 12,* 291–298. https://doi.org/10.1007/BF00884975.

El-Shakery, S. A., & Terauchi, Y. (1984). A computer-aided method for optimum design of plate cam-size avoiding undercutting and separation phenomena–II: Design nomograms. *Mechanism and Machine Theory, 19*(2), 235–241. https://doi.org/10.1016/0094-114X(84)90046-6.

Esmail, E. L. (2013). Nomographs for synthesis of epicyclic-type automatic transmissions. *Meccanica, 48,* 2037–2049. https://doi.org/10.1007/s11012-013-9721-z.

Esmail, E. L. (2016). Configuration design of ten-speed automatic transmissions with twelve-link three-DOF Lepelletier gear mechanism. *Journal of Mechanical Science and Technology, 30,* 211–220. https://doi.org/10.1007/s12206-015-1225-4.

Esmail, E. L. & Hussen, H. A. (2010). Nomographs for kinematics, statics and power flow analysis of epicyclic gear trains. In: Proceedings of the ASME 2009 International Mechanical Engineering Congress Exposition 13, (631–640). Lake Buena Vista, USA: ASME. https://doi.org/10.1115/IMECE2009-10789

Esmail, E. L., Pennestrì, E., & Juber, A. H. (2018). Power losses in two-degrees-of-freedom planetary gear trains: a critical analysis of Radzimovsky's formulas. *Mechanism and Machine Theory, 128,* 191–204. https://doi.org/10.1016/j.mechmachtheory.2018.05.015.

Evesham, H. A. (1986). Origins and development of nomography. *IEEE Annals of the History of Computing, 8*(4), 324–333. https://doi.org/10.1109/MAHC.1986.10059.

Evesham, H. A. (2010). *The history and development of nomography*. Docent Press http://hdl.handle.net/10547/581287.
Ferrara, G. E. (1940). Nomography for the electrical engineer. *Electrical Engineering, 59*(12), 505–508. https://doi.org/10.1109/EE.1940.6435199.
Gent, A. N. (1958). On the relation between indentation hardness and Young's modulus. *Rubber Chemistry and Technology, 31*(4), 896–906. https://doi.org/10.5254/1.3542351.
Glasser, L., & Doerfler, R. (2019). A brief introduction to nomography: Graphical representation of mathematical relationships. *International Journal of Mathematical Education in Science and Technology, 50*(8), 1273–1284. https://doi.org/10.1080/0020739X.2018.1527406.
Grier, D. A. (2001). Human computers: The first pioneers of the information age. *Endeavour, 25*(1), 28–32. https://doi.org/10.1016/S0160-9327(00)01338-7.
Grimes, D. A. (2008). The nomogram epidemic: Resurgence of a medical relic. *Annals of Internal Medicine, 149*(4), 273–275. https://doi.org/10.7326/0003-4819-149-4-200808190-00010.
Hain, K. (1961). Spring design and application. In N. P. Chironis (Ed.), *276, (274–275)*. McGraw-Hill, Inc.
Hankins, T. L. (1999). Blood, dirt, and nomograms: A particular history of graphs. *Isis, 90*(1), 50–80. https://doi.org/10.1086/384241.
Hassaan, G. A. (2015). Nomogram-based synthesis of complex planar mechanisms, part I: 6 bar-2 sliders mechanism. *International Journal of Engineering and Techniques, 1*(6), 29–35 https://scholar.cu.edu.eg/sites/default/files/galal/files/nomogram_pt_i.pdf.
Hilbert, D. (1901). Mathematische probleme. *Archive für Mathematik und Physik, 1*(1), 44–63.
Hilpert, H. (1968). Weight balancing of precision mechanical instruments. *Journal of Mechanisms, 3*(4), 289–302. https://doi.org/10.1016/0022-2569(68)90005-0.
Hohenberg, R. (1967). Detection and study of compressor-blade vibration. *Experimental Mechanics, 7,* 19A-24A. https://doi.org/10.1007/BF02327002.
Howison, M. (2014). Constructing interactive nomograms. https://www.researchgate.net/profile/Mark-Howison/publication/228841217_Constructing_Interactive_Nomograms/links/0fcfd50f99431f12e8000000/Constructing-Interactive-Nomograms.pdf
Hwang, W. M., & Chen, K. H. (2007). Triangular nomograms for symmetrical spherical non-Grashof double-rockers generating symmetrical coupler curves. *Mechanism and Machine Theory, 42*(7), 871–888. https://doi.org/10.1016/j.mechmachtheory.2006.05.008.
Kattan, M. W., & Marasco, J. (2010). What is a real nomogram? *Seminars in Oncology, 37*(1), 23–26. https://doi.org/10.1053/j.seminoncol.2009.12.003.
Khoshnevis, S., Brothers, R. M., & Diller, K. R. (2018). Level of cutaneous blood flow depression during cryotherapy depends on applied temperature: Criteria for protocol design. *ASME Journal of Medical Diagnostics, 1*(4), 041007. https://doi.org/10.1115/1.4041463.
Lu, D. M. (1999). A triangular nomogram for spherical symmetric coupler curves and its application to mechanism design. *Journal of Mechanical Design, 121*(2), 323–326. https://doi.org/10.1115/1.2829463.
Martínez-Pagán, P., & Roschier, L. (2022). Nomography: A renewed pedagogical tool to sciences and engineering high-education studies. *Heliyon, 8*(6), e09731. https://doi.org/10.1016/j.heliyon.2022.e09731.
Meyer zur Capellen, W. (1983). Nomogramme für die Krümmung sphärischer und ebener Bahnkurven. *Journal of Mechanism and Machine Theory, 18*(3), 249–254. https://doi.org/10.1016/0094-114X(83)90098-8.
Miconi, D. (1987). Vibration control in industrial plant: A methodological approach. *Journal of Vibration, Acoustics, Stress, and Reliability, 109*(4), 335–342. https://doi.org/10.1115/1.3269450.
Mottola, G. (2022) Scripts for paper "Nomograms in the history and education of machine mechanics". (online code repository). https://doi.org/10.5281/zenodo.7258700.
Mottola, G. & Cocconcelli, M. (2022). Nomograms: An old tool with new applications. In M. Ceccarelli & R. López-García (Eds), International Symposium on History of Machines and Mechanisms (pp.314–329). Jaén, Spain: Springer . https://doi.org/10.1007/978-3-030-98499-1_26.
Mottola, G., Cocconcelli, M., Rubini, R., & Carricato, M. (2022). Gravity compensation in robotics. In V. Arakelian (Ed.), *115* (pp. 229–273). Springer. https://doi.org/10.1007/978-3-030-95750-6_9.
Radaelli, G., Gallego, J. A., & Herder, J. L. (2011). An energy approach to static balancing of systems with torsion stiffness. *Journal of Mechanical Design, 133*(9), 091006. https://doi.org/10.1115/1.4004704.
Rusconi, F. (1962). Appunti di nomografia (E. Vandone, Ed). Milan: Etas Kompass.
Seireg, A. A., & Houser, D. R. (1970). Evaluation of dynamic factors for spur and helical gears. *Journal of Engineering for Industry, 92*(2), 504–514. https://doi.org/10.1115/1.3427790.
Soreau, R. (1902). Contributions à la théorie et aux applications de la nomographie. Paris: Beranger. https://babel.hathitrust.org/cgi/pt?id=mdp.39015038775394

Tournès, D. (2000). Notes & debats: Pour une histoire du calcul graphique. *Revue d'Histoire des Mathematiques, 6*(1), 127–161 http://www.numdam.org/item/RHM_2000__6_1_127_0/.
Tournès, D. (2003). Du compas aux intégraphes: les instruments du calcul graphique. *Repères-IREM, 50,* 63–84 https://publimath.univ-irem.fr/biblio/IWR03005.htm.
Tournès, D. (2014). Mathematik und Anwendungen. In M. Foote, M. Schmitz, B. Skorsetz, & R. Tobies (Eds.), *26–32*. ThILLM https://hal.univ-reunion.fr/hal-01187206.
Tournès, D., et al. (2018). Let history into the mathematics classroom. In Évelyne Barbin (Ed.), *101–114*. Springer. https://doi.org/10.1007/978-3-319-57150-8_8.
Warmus, M. (1959). Nomographic functions. Warsaw: Państwowe Wydawnictwo Naukowe.
Wegman, E. J. (1990). Hyperdimensional data analysis using parallel coordinates. *Journal of American Statistical Association, 85*(411), 664–675. https://doi.org/10.1080/01621459.1990.10474926.
Wellauer, E. J., & Holloway, G. A. (1976). Application of EHD oil film theory to industrial gear drives. *Journal of Engineering for Industry, 98*(2), 626–631. https://doi.org/10.1115/1.3438951.
Wunderlich, W. (1980). Nomogramme für die Wattsche Geradführung. *Mechanism and Machine Theory, 15*(1), 5–8. https://doi.org/10.1016/0094-114X(80)90028-2.
Young, W. C. & Budynas, R. G. (2002). Roark's formulas for stress and strain. McGraw-Hill.
Zotov, N. M., & Balakina, E. V. (2007). Using the φ- s^x nomogram in calculating the dynamics of a braked wheel. *Journal of Machinery Manufacture and Reliability, 36,* 193–198. https://doi.org/10.3103/S1052618807020161.

Giovanni Mottola was born in Italy on August 10, 1990. He received the M.S. degree in mechanical engineering and the Ph.D. degree in applied mechanics from the University of Bologna, Bologna, Italy, in 2015 and 2019, respectively. In 2017, he has been a visiting researcher at the Laval Robotics Laboratory at Université Laval (Québec, Canada). In 2020, he joined the University of Modena and Reggio Emilia, Reggio Emilia, Italy, where he is currently a Contract Researcher in applied mechanics in the Department of Sciences and Methods of Engineering. His research interests include parallel robots, machine diagnostics, and history of mechanical engineering.

Marco Cocconcelli was born in Italy on November 9, 1977. He received the M.S. degree in mechanical engineering and the Ph.D. degree in applied mechanics from the University of Bologna, Bologna, Italy, in 2003 and 2007, respectively. In 2007, he joined the University of Modena and Reggio Emilia, Reggio Emilia, Italy, where he is currently an associate professor in Applied Mechanics at the Department of Sciences and Methods for Engineering. His research interests include diagnostics of bearings and gears, condition monitoring of machinery, and history of mechanisms and machine science. He is a member of the Italian branch of the International Federation for the Promotion of Mechanism and Machine Science (IFToMM-Italy).